

## Quantum Monte Carlo simulation of BEC-impurity tunneling

A. S. Popova<sup>1,\*</sup>, V. V. Tiunova<sup>1</sup> and A. N. Rubtsov<sup>1,2</sup>

<sup>1</sup>*Russian Quantum Center, Bolshoy Bulvar 30, Building 1, Skolkovo, Moscow 121205, Russia*

<sup>2</sup>*Department of Physics, Lomonosov Moscow State University, Leninskie gory 1, Moscow 119991, Russia*



(Received 23 November 2020; revised 1 March 2021; accepted 31 March 2021; published 9 April 2021)

Polaron tunneling is a prominent example of a problem characterized by different energy scales, for which the standard quantum Monte Carlo methods face a slowdown problem. We propose a quantum-tunneling Monte Carlo (QPMC) method which is free from this issue and can be used for a wide range of tunneling phenomena. We apply it to study an impurity interacting with a one-dimensional Bose-Einstein condensate and simultaneously trapped in an external double-well potential. Our scheme works for an arbitrary coupling between the particle and condensate and, at the same time, allows for an account of tunneling effects. We discover two distinct quasiparticle peaks associated, respectively, with the phonon-assisted tunneling and the self-trapping of the impurity, which are in a crossover regime for the system modeled. We observe and analyze changes in the weights and spectral positions of the peaks (or, equally, effective masses of the quasiparticles) when the coupling strength is increased. Possible experimental realizations using cold atoms are discussed.

DOI: [10.1103/PhysRevB.103.155406](https://doi.org/10.1103/PhysRevB.103.155406)

### I. INTRODUCTION

The dynamics of a single mobile impurity interacting with a reservoir is one of the fundamental problems in condensed matter physics. The corresponding model, the so-called polaron model, was introduced to describe the coupling between electrons and lattice phonons in a dielectric crystal [1]. Nowadays, the polaronic effects have been extensively studied for impurities in Bose-Einstein condensates (BECs) [2–5], where a tunable interaction between impurities and host atoms via the Feshbach resonance goes beyond the parameter range relevant for solids [6]. However, theoretical techniques based on perturbation theory [7,8] and variational approaches [9–13] result in different predictions at the strong interaction even for the one dimensional polarons [14]. Nevertheless, this model became a sound benchmark for various many-body techniques [6,15] with an unprecedented opportunity for their experimental testing [16–19]. The transport of impurities interacting with a many-body environment has been also investigated in optical lattices [20–24]. Apart from that, progress in this area is also important for a deeper understanding of the physics of neutral atoms in optical traps [25,26] and quantum dots [27,28], especially in the context of quantum information theory.

Generally, the incoherent tunneling effect [29,30] with a nonlinear coupling is hard to study with analytical and numerical approaches. A tunneling particle interacting with a bath has at least two different energy scales—a barrier height (related to the tunneling energy splitting) and the interaction strength. Path-integral quantum Monte Carlo (QMC) methods can be applied to this problem since they are commonly used to study quantum impurity models [31,32]. Moreover, the

QMC studies of tunneling processes have gained an increased interest in the field of adiabatic quantum computing [33,34]. However, the straightforward application of the QMC algorithm for the simulation of tunneling is limited by its high computational complexity [35–38]. This slowdown problem is related to a complex energy landscape for the Feynman path integral.

In this paper, we propose a special modification of the path-integral QMC method for incoherent impurity tunneling and apply it to the polaron problem. We investigate tunneling of a single impurity immersed in a one-dimensional BEC and trapped in a double-well potential. Our method is based on splitting the path-integral computation into two independent parts. The first one corresponds to the process of tunneling through a double-well barrier, which can be efficiently estimated, and the second one corresponds to a retarded interaction with the bath. We consider a particle in a double-well potential in a numerically exact way, and BEC excitations are determined by integrating out the bosonic modes. The method relies on the assumption that the typical energy of the BEC-impurity interaction is comparable with the tunnel splitting, but much smaller than the barrier height. By performing an analytical continuation of the computed impurity's correlation functions, we calculate the density of states for different interaction strengths in the low-temperature limit. Moreover, we identify emergent peaks in the density of states as quasiparticle peaks and estimate their effective mass. Using the proposed QMC method, we discover the crossover in the BEC-impurity system from phonon-assisted tunneling [39,40] at a weak coupling to self-trapping in a strong interaction case [41].

The paper is organized as follows. In Sec. II we discuss the general formalism as well as the model and the proposed method. Section III contains details of the proposed QMC scheme for the BEC-polaron tunneling in the case of

\*chertkova.anastasia.phys@gmail.com

a two-mode bath, a comparison with the exact diagonalization method, and results for a model with the continuous spectrum of the bath. We provide conclusions in Sec. IV.

## II. MODEL AND METHOD

### A. Fröhlich-Bogoliubov model

We use the Fröhlich Hamiltonian, which describes the impurity in a Bose-Einstein condensate in the Bogoliubov approximation [2,3,9],

$$\hat{H}_{\text{FB}} = \frac{\hat{p}^2}{2m_I} + \sum_{k \neq 0} \hbar \omega_k \hat{b}_k^\dagger \hat{b}_k + \sum_{k \neq 0} (V_k e^{-ik\hat{x}} \hat{b}_{-k} + \text{H.c.}),$$

$$V_k = \frac{a_{IB} \sqrt{n_0}}{\sqrt{2\pi M}} \left[ \frac{(\xi k)^2}{2 + (\xi k)^2} \right]^{1/4} \omega_k = ck \left[ 1 + \frac{(\xi k)^2}{2} \right]^{1/2}, \quad (1)$$

where  $\hat{p}$  and  $\hat{x}$  are momentum and position operators of the impurity atom with mass  $m_I$ ,  $\hat{b}_k^\dagger$  is the creation operator of the Bogoliubov excitation with momentum  $k$  and frequency  $\omega_k$ ,  $V_k$  is the interaction strength of phonon modes with the impurity atom,  $c$  and  $\xi$  are the speed of sound in BEC and its healing length, respectively,  $a_{IB}$  is the boson-impurity scattering length,  $n_0$  is the BEC density, and  $M^{-1} = m_B^{-1} + m_I^{-1}$  is the reduced mass, where  $m_B$  is the mass of a host atom.

To study the equilibrium properties of the polaron tunneling we consider the impurity in the double-well potential,

$$\hat{H} = \hat{H}_{\text{FB}} + \kappa \left( -\frac{\hat{x}^2}{2} + \frac{\hat{x}^4}{4} \right), \quad (2)$$

where we set  $\hbar$ ,  $e$ ,  $d$  to unity ( $e = c/\xi$  is the energy in the polaronic units [11], and  $2d$  is the distance between wells of the double-well potential).

### B. Quantum-tunneling Monte Carlo method

The Feynman path integral defines a transition amplitude as a sum of all possible paths between given initial and final configurations of a quantum system. The standard path-integral quantum Monte Carlo method utilizes this idea in a sampling of a large number of discrete trajectories in imaginary time [42]. On every step of the algorithm, the current trajectory is changed according to the Metropolis condition [43]. As more steps of the method are applied, the closer the result becomes to the exact one.

For tunneling problems with multiple minima of the energy landscape the standard QMC sampling of valuable trajectories leads to the exponential growth of computational time [36–38,44]. In other words, the standard path-integral QMC cannot reach any stable result in a reasonable amount of time. The reason for the QMC scheme failure is that the tunneling time is much larger than the timescale of the interaction. For BEC, this gives  $\hbar/\kappa \ll \hbar M/a_{IB} \sqrt{n_0}$ , and as a consequence, the calculation requires a very fine grid for the trajectories. To overcome this problem, we proposed another algorithm—the quantum-tunneling Monte Carlo method (QTMC). Our approach separates the path-integral computation into two parts. The impurity tunneling in a double-well contribution is accounted for through a numerically exact calculation of its propagator and the BEC excitations are integrated out in the

low-temperature limit, which results in the following retarded action,

$$Z = \int \mathcal{D}[x, b^\dagger, b] e^{-S[x, b^\dagger, b]} = \int \mathcal{D}[x] e^{-S_I[x]} e^{-S_R[x]},$$

$$e^{-S_R[x]} \equiv \int \mathcal{D}[b^\dagger, b] e^{-S_B[x, b^\dagger, b]}, \quad (3)$$

where  $S_I[x]$  is the action of the impurity in a double-well potential,  $S_B[x]$  is the action related to the impurity in the BEC, and  $S_R[x]$  is the retarded polaronic action,

$$S_R = -2 \sum_{k \neq 0} V_k^2 \sum_{\tau, \tau'} e^{-ik(x(\tau) - x(\tau'))}$$

$$\times \frac{e^{-\omega_k[(\tau - \tau') + \beta \Theta(-(\tau - \tau'))]}}{1 - e^{-\omega_k \beta}} \delta\tau \delta\tau', \quad (4)$$

where  $\Theta(\tau)$  is the Heaviside step function,  $\beta$  is an inverse temperature, and  $\delta\tau$  is a time slice.

The action of the impurity  $S_I[x]$  can be defined through the Feynman propagator—the probability amplitude to find a particle at the position  $x'$  from  $x$  in the time interval  $\delta\tau$  [45]. We exactly diagonalize the Hamiltonian for the particle in the double-well potential and obtain the eigenfunctions and eigenvalues  $\phi_i$ ,  $E_i$  to estimate the propagator via

$$K(x, x', \delta\tau) = \sum_i \phi_i^*(x) \phi_i(x') e^{-E_i \delta\tau}. \quad (5)$$

We use the finite-difference method to compute the eigenfunctions and eigenvalues  $\phi_i$ ,  $E_i$ .

Now we discuss the algorithm of the QTMC procedure in more detail: (1) an explicit calculation of the propagator of the noninteracting impurity  $K(x', x, \tau)$  in a numerically exact way; (2) a numerical evaluation of the retarded action  $S_R$  for different values of  $x(\tau) - x(\tau')$ ; and (3) a Monte Carlo sampling of the impurity's trajectories using the calculated propagator  $K(x', x, \tau)$  and the retarded action  $S_R$ .

Thus, we reduce the initial many-body problem to a single-particle problem with the effective retarded action, which includes correlations of all orders in a numerically exact way. Our QTMC scheme samples the impurity trajectories in imaginary time with periodic boundary conditions on a coarse time grid with the step  $\delta\tau \sim \Delta E^{-1}$ .

We apply the QTMC algorithm to find the correlation functions  $\langle x_0 x_\tau \rangle$  of the impurity in the imaginary time. Using the QTMC data, we obtain a density of states (DOS) on a real axis through a Fourier transform [46,47],

$$\langle x_0 x_\tau \rangle = \frac{1}{2\pi} \int_0^\infty \frac{e^{-\omega\tau} + e^{-\omega(\beta-\tau)}}{1 - e^{-\omega\beta}} \rho(\omega) d\omega. \quad (6)$$

The integral (6) is restricted to the positive frequencies  $\omega$ , which is possible since  $\langle x_0 x_\tau \rangle = \langle x_0 x_{\beta-\tau} \rangle$  [47].

We note that there are certain similarities between our approach and the strategy used in Refs. [48–50] to simulate hard-core interactions in quantum bosonic fluids. In these works, the exact propagators for the single particle in a trap are also used for the effective sampling of configurations. However, we stress that Refs. [48–50] use the two-particle approximation for the density matrix, whereas our approach is formally numerically exact and preserves correlations at all orders.

### C. Maximum entropy method

Generally, finding the analytical continuation  $\rho(\omega)$  from the imaginary-time Green's function  $\langle x_0 x_\tau \rangle$  is an ill-conditioned problem [51], i.e., the solution is highly sensitive to noise of the input data. The maximum entropy method (MaxEnt) is a widely used approach to extract the analytical continuation  $\rho(\omega)$  from the correlation functions  $\langle x_0 x_\tau \rangle$ . The main idea of the MaxEnt method is to minimize the cost function  $\frac{1}{2}\chi - \alpha S[\rho]$ , where  $\chi$  is the quadratic loss function of  $\langle x_0 x_\tau \rangle$ ,  $S[\rho]$  is the Shannon entropy term, and  $\alpha$  is a regularization parameter [47]. The distribution that maximizes the information entropy is the one that is statistically most favored [52]. In other words, the less known about a target spectral function  $\rho(\omega)$ , the higher is its Shannon entropy. The proper initial guess for the distribution—the default model—helps to reconstruct the unique analytical continuation. Thus, solving the nonlinear optimization problem, we find a finite, smooth, and positive spectral function  $\rho(\omega)$  without overfitting the correlation function's noise [46].

### III. RESULTS

Here, we present the numerical results for the system with the parameters corresponding to a  $^{39}\text{K}$  tunneling impurity in the  $^{87}\text{Rb}$  condensate. First, we benchmark the proposed quantum-tunneling Monte Carlo algorithm on the model (2) with the two resonance modes of the Bogoliubov excitations. We solve this problem by the exact diagonalization (ED) method and the QTMC scheme [with ten eigenfunctions  $\phi_i$  held in Eq. (5)] for the different coupling strengths or equivalently the boson-impurity scattering lengths  $a_{IB}$  (see Fig. 1). The exact diagonalization algorithm provides the solution as a set of delta-function peaks for this problem. In Fig. 1 these peaks are slightly broadened for easier visualization. The QTMC correlation functions  $\langle x_0 x_\tau \rangle$  were transformed into the density of states by the MaxEnt method. This procedure approximates the DOS by Gaussian peaks of a fixed width, defined by the accuracy of QTMC calculations. Nevertheless, significant features of the density of states, namely a peak position and its amplitude, can be obtained without any restrictions on the boson-impurity scattering length  $a_{IB}$ . We note that the calculation time slightly grows with the coupling  $a_{IB}$  since it is necessary to use a finer time grid in the strong-coupling regime.

For a free impurity in the double-well potential, we find a single peak in the DOS, corresponding to the tunneling splitting  $\Delta E$  [Fig. 1(a)]. At the small coupling, this peak splits into two [Fig. 1(b)]. As the interaction grows, the right peak shifts to the higher frequencies and its amplitude decreases, while the left DOS peak grows higher and shifts to the lower frequencies. Finally, the lower-energy peak dominates for strong coupling, which might indicate a self-trapping of the impurity [Fig. 1(c)]. There are slight differences in  $\rho(\omega)$  between the ED and QTMC peaks due to the finite accuracy of the MaxEnt procedure (see Sec. II C for details). Also, our scheme cannot resolve the smallest DOS peaks for the strong coupling [Fig. 1(c)], but we believe that these peaks do not significantly influence the impurity tunneling.

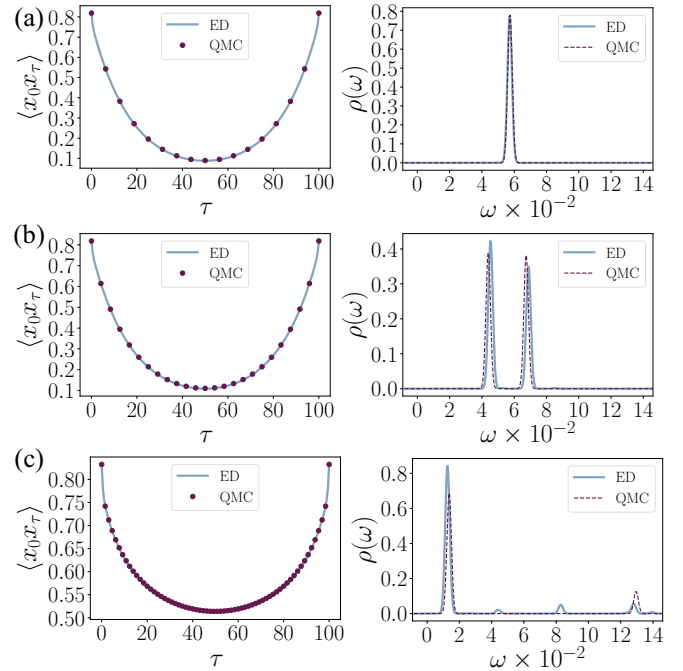


FIG. 1. Correlation functions  $\langle x_0 x_\tau \rangle$  and spectral densities of states  $\rho(\omega)$  for a  $^{39}\text{K}$  impurity, which interacts with the two resonance modes of Bogoliubov excitations ( $k = \pm 0.805$ ,  $\omega_k = \Delta E \sim 0.057$ ) of the  $^{87}\text{Rb}$  condensate (the healing length  $\xi = 2.5$ ) and trapped in a double-well potential with  $\kappa = 10.24$  for different values of the scattering length: (a)  $a_{IB} = 0.0$ , (b)  $a_{IB} = 0.08$ , and (c)  $a_{IB} = 0.34$ . Dotted and dashed lines correspond to the QTMC simulation with  $10^{10}$  steps, and solid lines are the exact diagonalization results,  $\beta = 100$ .

Now let us discuss the QTMC results for the model (2) of the  $^{39}\text{K}$  tunneling impurity with the continuous bosonic spectrum of Bogoliubov excitations (the healing length  $\xi = 2.5$ , and the inverse temperature  $\beta = 100$  corresponding to  $T = 160$  nK), which does not allow the ED treatment. Figure 2 shows the obtained spectral density of the states from the QTMC data. The spectrum of the bosonic modes was cut off at  $k_{\max} = 1.5$ , which corresponds to the frequency cut  $\omega(k_{\max}) = 3\Delta E$ . We checked that the obtained results do not depend on the specific choice of the cut. The DOS behavior is qualitatively similar to that of the two-mode problem. There is a single DOS peak for zero coupling, which is related to the energy level splitting for the particle in a double-well potential  $\omega_0 = \Delta E$  (vertical line in Fig. 2). In other words, a particle is tunneling from one well of the potential to another for tunneling time  $t = \pi/\Delta E$ . For a small interaction strength (scattering length  $a_{IB} < 0.04$ ), the tunneling DOS peak shifts to higher frequencies, and another small DOS peak appears. The amplitude of the right DOS peak decreases with coupling, but its position continues to move to higher frequencies, which means the decreasing impurity tunneling time in the presence of resonant phonons, i.e., phonon-assisted tunneling. Simultaneously, the left DOS peak grows and shifts to lower frequencies. For the scattering length  $a_{IB} > 0.06$ , this peak becomes a dominating feature of the DOS, i.e., the tunneling time grows (Fig. 2). It means that the impurity does not

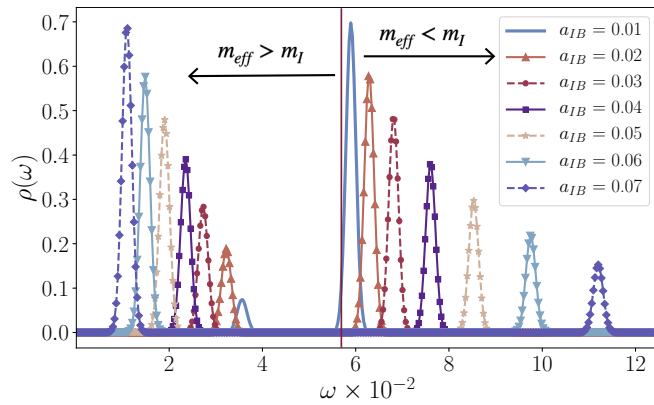


FIG. 2. Spectral densities of states  $\rho(\omega)$  for a  $^{39}\text{K}$  tunneling impurity, which interacts with the continuous spectrum of Bogoliubov excitations in the  $^{87}\text{Rb}$  condensate (the healing length  $\xi = 2.5$ ),  $\kappa = 10.24$ ,  $\beta = 100$ ,  $10^{10}$  QTMC steps. The vertical line corresponds to the tunneling energy splitting for zero interaction  $a_{IB} = 0$ .

transfer into another well of the potential or, in other words, it is self-trapped in the strong interaction regime. This process is interpreted as the formation of a heavy phonon cloud around the particle at which a bound state of the impurity emerges.

For the obtained QTMC data, the MaxEnt method does not signal any change in the widths of the DOS peaks. Since the DOS peaks are narrow, we can interpret them as quasiparticle peaks and define their effective masses as functions of scattering length (Fig. 3). For a given double-well potential (with  $\kappa = 10.24$  in our case), we can employ the exact diagonalization to obtain a dependence of the tunneling splitting  $\Delta E$  on a particle mass. This dependence can be used to estimate an effective mass for each DOS peak. We see that for a small interaction strength, which we refer to as a phonon-assisted tunneling region, the effective mass decreases (circles in Fig. 3). For large coupling, we observe an increase of the effective mass, which indicates that the impurity is localized in this regime (squares in Fig. 3). In the intermediate case, there is a crossover region, where two DOS peaks have nearly

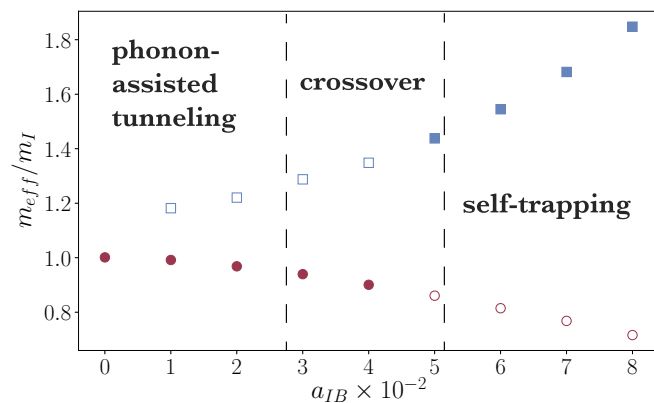


FIG. 3. Effective mass corresponding to the quasiparticle peaks of the density of states for a  $^{39}\text{K}$  tunneling impurity in the  $^{87}\text{Rb}$  condensate (the healing length  $\xi = 2.5$ ); circles represent the higher-frequency peaks, squares the lower-frequency ones; solid (open) marks are dominant (lesser) peaks;  $\kappa = 10.24$ ,  $\beta = 100$ .

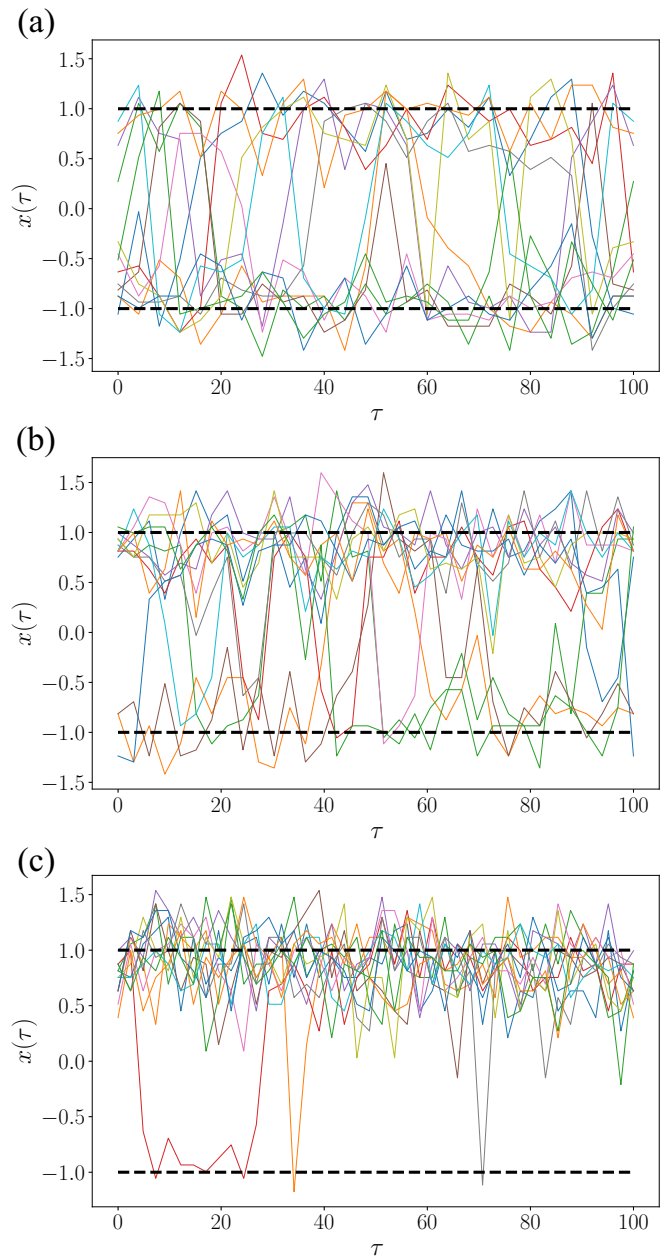


FIG. 4. Impurity trajectories  $x(\tau)$  in imaginary time for different values of interaction strength with the  $^{87}\text{Rb}$  condensate (the healing length  $\xi = 2.5$ ): (a)  $a_{IB} = 0.01$ , (b)  $a_{IB} = 0.05$ , and (c)  $a_{IB} = 0.09$ ; dashed lines correspond to the minima of the double-well potential,  $\kappa = 10.24$ ,  $\beta = 100$ .

the same amplitude, and these two phenomena coexist. We emphasize that the defined effective masses are not directly related to the impurity effective mass in the BEC in the absence of the tunneling potential [32] and further investigation is needed to elaborate on their connection.

In Fig. 4 we also show the sampled imaginary-time trajectories for the different scattering lengths  $a_{IB}$ . For a small interaction strength, the impurity tunnels freely from one well to another [Fig. 4(a)]. In the crossover region, the impurity tunneling starts to lessen, which results in a slightly asymmetric probability distribution [Fig. 4(b)]. For a

strong coupling, the tunneling process is almost suppressed, which indicates the self-trapping of the impurity in one of the wells [Fig. 4(c)].

#### IV. CONCLUSIONS

In the present work we propose a special modification of the quantum Monte Carlo method for the tunneling problems (QTMC) in an external environment, which can simulate equilibrium dynamics beyond perturbation theory. The QTMC scheme enables us to investigate how the bosonic bath affects tunneling without an exponential slowdown usual for the standard QMC method. We apply this approach to study the tunneling of the BEC impurity in one dimension in the Fröhlich-Bogolubov approximation. The impurity's correlation functions were calculated by the QTMC scheme and transformed into the density of states using the MaxEnt procedure. We verified our method by employing exact diagonalization for the model bath with two resonance modes of the bosonic field.

For the continuous bosonic spectrum, we found that the BEC impurity undergoes a crossover between the

phonon-assisted tunneling at the weak coupling and self-trapping for the strong interaction. Also, we found the quasiparticle peaks in DOS and estimate their effective mass. These phenomena might be observed in the recent experiment realization [16,17] with an addition of two close harmonic optical dipole traps for the impurity [53,54]. A spectral response of the tunneling impurity in the BEC on radio-frequency pulses might be used for the observation of the crossover between the phonon-assisted tunneling and the self-trapping regimes. Moreover, it was shown that the inhomogeneous BEC could produce the effective double-well potential for the impurity during quench dynamics [55,56]. These works motivate a further study of the dynamical phenomena in the explored BEC-impurity model and its extensions.

#### ACKNOWLEDGMENTS

The authors thank E. A. Polyakov for useful discussions. A.S.P. acknowledges the support by Theoretical Physics and Mathematics Advancement Foundation "BASIS" through Grant No. 19-2-6-241-1. V.V.T. acknowledges the support by Russian Science Foundation through Grant No. 19-71-10092.

- 
- [1] L. Landau and S. Pekar, Effective mass of a polaron, *Zh. Eksp. Teor. Fiz.* **18**, 419 (1948).
  - [2] F. M. Cucchiatti and E. Timmermans, Strong-Coupling Polarons in Dilute Gas Bose-Einstein Condensates, *Phys. Rev. Lett.* **96**, 210401 (2006).
  - [3] K. Sacha and E. Timmermans, Self-localized impurities embedded in a one-dimensional Bose-Einstein condensate and their quantum fluctuations, *Phys. Rev. A* **73**, 063604 (2006).
  - [4] J. Levinsen, M. M. Parish, and G. M. Bruun, Impurity in a Bose-Einstein Condensate and the Efimov Effect, *Phys. Rev. Lett.* **115**, 125302 (2015).
  - [5] F. Grusdt and M. Fleischhauer, Tunable Polarons of Slow-Light Polaritons in a Two-Dimensional Bose-Einstein Condensate, *Phys. Rev. Lett.* **116**, 053602 (2016).
  - [6] M. Drescher, M. Salmhofer, and T. Enss, Real-space dynamics of attractive and repulsive polarons in Bose-Einstein condensates, *Phys. Rev. A* **99**, 023601 (2019).
  - [7] S. P. Rath and R. Schmidt, Field-theoretical study of the Bose polaron, *Phys. Rev. A* **88**, 053632 (2013).
  - [8] R. S. Christensen, J. Levinsen, and G. M. Bruun, Quasiparticle Properties of a Mobile Impurity in a Bose-Einstein Condensate, *Phys. Rev. Lett.* **115**, 160401 (2015).
  - [9] J. Tempere, W. Casteels, M. K. Oberthaler, S. Knoop, E. Timmermans, and J. T. Devreese, Feynman path-integral treatment of the BEC-impurity polaron, *Phys. Rev. B* **80**, 184504 (2009).
  - [10] W. Casteels, J. Tempere, and J. T. Devreese, Polaronic properties of an impurity in a Bose-Einstein condensate in reduced dimensions, *Phys. Rev. A* **86**, 043614 (2012).
  - [11] F. Grusdt, Y. E. Shchadilova, A. N. Rubtsov, and E. Demler, Renormalization group approach to the Fröhlich polaron model: Application to impurity-BEC problem, *Sci. Rep.* **5**, 12124 (2015).
  - [12] Y. E. Shchadilova, R. Schmidt, F. Grusdt, and E. Demler, Quantum Dynamics of Ultracold Bose Polarons, *Phys. Rev. Lett.* **117**, 113002 (2016).
  - [13] A. G. Volosniev and H.-W. Hammer, Analytical approach to the Bose-polaron problem in one dimension, *Phys. Rev. A* **96**, 031601(R) (2017).
  - [14] F. Grusdt, G. E. Astrakharchik, and E. Demler, Bose polarons in ultracold atoms in one dimension: Beyond the Fröhlich paradigm, *New J. Phys.* **19**, 103035 (2017).
  - [15] S. I. Mistakidis, A. G. Volosniev, N. T. Zinner, and P. Schmelcher, Effective approach to impurity dynamics in one-dimensional trapped Bose gases, *Phys. Rev. A* **100**, 013619 (2019).
  - [16] N. B. Jørgensen, L. Wacker, K. T. Skalmstang, M. M. Parish, J. Levinsen, R. S. Christensen, G. M. Bruun, and J. J. Arlt, Observation of Attractive and Repulsive Polarons in a Bose-Einstein Condensate, *Phys. Rev. Lett.* **117**, 055302 (2016).
  - [17] M.-G. Hu, M. J. Van de Graaff, D. Kedar, J. P. Corson, E. A. Cornell, and D. S. Jin, Bose Polarons in the Strongly Interacting Regime, *Phys. Rev. Lett.* **117**, 055301 (2016).
  - [18] L. A. Pena Ardila and S. Giorgini, Bose polaron problem: Effect of mass imbalance on binding energy, *Phys. Rev. A* **94**, 063640 (2016).
  - [19] S. I. Mistakidis, G. C. Katsimiga, G. M. Koutentakis, T. Busch, and P. Schmelcher, Pump-probe spectroscopy of Bose polarons: Dynamical formation and coherence, *Phys. Rev. Research* **2**, 033380 (2020).
  - [20] M. Bruderer, A. Klein, S. R. Clark, and D. Jaksch, Transport of strong-coupling polarons in optical lattices, *New J. Phys.* **10**, 033015 (2008).
  - [21] Z. Cai, L. Wang, X. C. Xie, and Y. Wang, Interaction-induced anomalous transport behavior in one-dimensional optical lattices, *Phys. Rev. A* **81**, 043602 (2010).

- [22] T. H. Johnson, S. R. Clark, M. Bruderer, and D. Jaksch, Impurity transport through a strongly interacting bosonic quantum gas, *Phys. Rev. A* **84**, 023617 (2011).
- [23] F. Theel, K. Keiler, S. I. Mistakidis, and P. Schmelcher, Many-body collisional dynamics of impurities injected into a double-well trapped Bose-Einstein condensate, [arXiv:2009.12147](https://arxiv.org/abs/2009.12147).
- [24] S. Palzer, C. Zipkes, C. Sias, and M. Köhl, Quantum Transport Through a Tonks-Girardeau Gas, *Phys. Rev. Lett.* **103**, 150601 (2009).
- [25] D. Frese, B. Ueberholz, S. Kuhr, W. Alt, D. Schrader, V. Gomer, and D. Meschede, Single Atoms in an Optical Dipole Trap: Towards a Deterministic Source of Cold Atoms, *Phys. Rev. Lett.* **85**, 3777 (2000).
- [26] H. Bernien, S. Schwartz, A. Keesling, H. Levine, A. Omran, H. Pichler, S. Choi, A. S. Zibrov, M. Endres, M. Greiner *et al.*, Probing many-body dynamics on a 51-atom quantum simulator, *Nature (London)* **551**, 579 (2017).
- [27] T. Stauber, R. Zimmermann, and H. Castella, Electron-phonon interaction in quantum dots: A solvable model, *Phys. Rev. B* **62**, 7336 (2000).
- [28] D. Loss and D. P. DiVincenzo, Quantum computation with quantum dots, *Phys. Rev. A* **57**, 120 (1998).
- [29] U. Weiss, H. Grabert, P. Hänggi, and P. Riseborough, Incoherent tunneling in a double well, *Phys. Rev. B* **35**, 9535 (1987).
- [30] S. V. Isakov, G. Mazzola, V. N. Smelyanskiy, Z. Jiang, S. Boixo, H. Neven, and M. Troyer, Understanding Quantum Tunneling Through Quantum Monte Carlo Simulations, *Phys. Rev. Lett.* **117**, 180402 (2016).
- [31] F. Lingua, B. Capogrosso-Sansone, A. Safavi-Naini, A. J. Jahangiri, and V. Penna, Multiworm algorithm quantum Monte Carlo, *Phys. Scr.* **93**, 105402 (2018).
- [32] L. A. Pena Ardila and S. Giorgini, Impurity in a Bose-Einstein condensate: Study of the attractive and repulsive branch using quantum Monte Carlo methods, *Phys. Rev. A* **92**, 033612 (2015).
- [33] E. M. Inack and S. Pilati, Simulated quantum annealing of double-well and multiwell potentials, *Phys. Rev. E* **92**, 053304 (2015).
- [34] L. Stella, G. E. Santoro, and E. Tosatti, Monte Carlo studies of quantum and classical annealing on a double well, *Phys. Rev. B* **73**, 144302 (2006).
- [35] L. A. Pena Ardila, N. B. Jørgensen, T. Pohl, S. Giorgini, G. M. Bruun, and J. J. Arlt, Analyzing a Bose polaron across resonant interactions, *Phys. Rev. A* **99**, 063607 (2019).
- [36] E. Gull, A. J. Millis, A. I. Lichtenstein, A. N. Rubtsov, M. Troyer, and P. Werner, Continuous-time Monte Carlo methods for quantum impurity models, *Rev. Mod. Phys.* **83**, 349 (2011).
- [37] E. M. Inack, G. Giudici, T. Parolini, G. Santoro, and S. Pilati, Understanding quantum tunneling using diffusion Monte Carlo simulations, *Phys. Rev. A* **97**, 032307 (2018).
- [38] N. Nemeč, Diffusion Monte Carlo: Exponential scaling of computational cost for large systems, *Phys. Rev. B* **81**, 035119 (2010).
- [39] D. Y. Oberli, J. Shah, T. C. Damen, J. M. Kuo, J. E. Henry, J. Lary, and S. M. Goodnick, Optical phonon-assisted tunneling in double quantum well structures, *Appl. Phys. Lett.* **56**, 1239 (1990).
- [40] V. Vargas-Calderón and H. Vinck-Posada, Light emission properties in a double quantum dot molecule immersed in a cavity: Phonon-assisted tunneling, *Phys. Lett. A* **384**, 126076 (2020).
- [41] A. E. Myasnikova, Band structure in autolocalization and bipolaron models of high-temperature superconductivity, *Phys. Rev. B* **52**, 10457 (1995).
- [42] M. J. E. Westbroek, P. R. King, D. D. Vvedensky, and S. Dürr, User's guide to Monte Carlo methods for evaluating path integrals, *Am. J. Phys.* **86**, 293 (2018).
- [43] N. Metropolis and S. Ulam, The Monte Carlo method, *J. Am. Stat. Assoc.* **44**, 335 (1949).
- [44] T. Parolini, E. M. Inack, G. Giudici, and S. Pilati, Tunneling in projective quantum Monte Carlo simulations with guiding wave functions, *Phys. Rev. B* **100**, 214303 (2019).
- [45] R. P. Feynman, A. R. Hibbs, and D. F. Styer, *Quantum Mechanics and Path Integrals* (Courier Corporation, North Chelmsford, MA, 2010).
- [46] R. Levy, J. P. F. LeBlanc, and E. Gull, Implementation of the maximum entropy method for analytic continuation, *Comput. Phys. Commun.* **215**, 149 (2017).
- [47] M. Jarrell and J. E. Gubernatis, Bayesian inference and the analytic continuation of imaginary-time quantum Monte Carlo data, *Phys. Rep.* **269**, 133 (1996).
- [48] S. Pilati, K. Sakkos, J. Boronat, J. Casulleras, and S. Giorgini, Equation of state of an interacting Bose gas at finite temperature: A path-integral Monte Carlo study, *Phys. Rev. A* **74**, 043621 (2006).
- [49] D. M. Ceperley, Path integrals in the theory of condensed helium, *Rev. Mod. Phys.* **67**, 279 (1995).
- [50] W. Krauth, Quantum Monte Carlo Calculations for a Large Number of Bosons in a Harmonic Trap, *Phys. Rev. Lett.* **77**, 3695 (1996).
- [51] H. Yoon, J.-H. Sim, and M. J. Han, Analytic continuation via domain knowledge free machine learning, *Phys. Rev. B* **98**, 245101 (2018).
- [52] L. R. Mead and N. Papanicolaou, Maximum entropy in the problem of moments, *J. Math. Phys.* **25**, 2404 (1984).
- [53] N. Spethmann, F. Kindermann, S. John, C. Weber, D. Meschede, and A. Widera, Dynamics of Single Neutral Impurity Atoms Immersed in an Ultracold Gas, *Phys. Rev. Lett.* **109**, 235301 (2012).
- [54] J. Catani, G. Lamporesi, D. Naik, M. Gring, M. Inguscio, F. Minardi, A. Kantian, and T. Giamarchi, Quantum dynamics of impurities in a one-dimensional Bose gas, *Phys. Rev. A* **85**, 023623 (2012).
- [55] S. I. Mistakidis, G. M. Koutentakis, G. C. Katsimiga, T. Busch, and P. Schmelcher, Many-body quantum dynamics and induced correlations of Bose polarons, *New J. Phys.* **22**, 043007 (2020).
- [56] S. I. Mistakidis, G. C. Katsimiga, G. M. Koutentakis, T. Busch, and P. Schmelcher, Quench Dynamics and Orthogonality Catastrophe of Bose Polarons, *Phys. Rev. Lett.* **122**, 183001 (2019).